Empirically assessing the potential release of rare earth elements from black shale under simulated hydraulic fracturing conditions

Jon Yang[1], Circe Verba[2*], Marta Torres[1], J. Alexandra Hakala[3]

[1]College of Earth, Ocean, and Atmospheric Sciences, Oregon State University, Corvallis, OR 97331-5503

[2]Research and Innovation Center, National Energy Technology Laboratory, US Department of Energy, Albany, OR 97321

[3]Research and Innovation Center, National Energy Technology Laboratory, US Department of Energy, Pittsburgh, PA 10940

*Corresponding author

ABSTRACT

Rare earth elements (REEs) are economically important to modern society and the rapid growth of technologies dependent on REEs has placed considerable economic pressure on their sourcing. This study addresses whether REEs could be released as a byproduct of natural gas extraction from a series of experiments that were designed to simulate hydraulic fracturing of black shale under various pressure (25 and 27.5 MPa) and temperature (50, 90, 130 ^{o}C) conditions. The dissolved REEs in the reacted fluids displayed no propensity for the REEs to be released from black shale under high pressure and temperature conditions, a result that is consistent across the different types of fluids investigated. Overall, there was a net loss of REEs from the fluid. These changes in dissolved REEs were greatest at the moment the fluids first contacted the shale and before the high temperature and high pressure conditions were imposed, although the magnitude of these changes (10^{-4} µg/g) were small compared to the magnitude of the total REE content present in the solid shale samples (10^{2} µg/g). These results highlight the variability and complexity of hydraulic fracturing systems and indicate that REE may not serve as robust tracers for fracturing fluid-shale reactions. Additionally, the results suggest that significant quantities of REEs may not be byproducts of hydraulically fractured shales.

Keywords: rare earth elements, hydraulic fracturing, rocking autoclave, Marcellus Shale

1. INTRODUCTION

The fourteen naturally occurring rare earth elements (REEs) of the lanthanide series are vital components in modern technology. Various REEs (e.g. Nd, Dy) are utilized in commercial applications such as computer chips, high-energy lasers, batteries, and green technologies (e.g., Alonso et al., 2012). Locating alternative sources of REEs is thus valuable to relieve the demand in the global market. Organic-rich black shale formations may present an intriguing potential source for REEs. Black shales are formed in marine environments under reducing conditions and the high accumulation of organic matter typical of these deposits can later be converted to natural gas and oil under high pressure and temperature (McCarthy et al., 2011). The average REE content of black shales is on the order of 180 ppm (Taylor and McLennan, 1985). Comparatively, economic deposits of REEs within bastnasite ores on average contain 70 wt% of rare earth oxides (~ 7 x 10^5 ppm) (Long et al., 2012). While black shales are not traditionally considered economic deposits of REEs, these shales are nevertheless important resources for natural gas and oil; subsequently, REEs could potentially constitute a byproduct of drilling operations (Alexander et al., 2011; Engelder, 2009; Kargbo et al., 2010).

During natural gas extraction from black shale formations, drilling operators inject millions of gallons of water into the shale formation under high pressures to create fractures and fissures for natural gas to flow freely to the surface in a process known as hydraulic fracturing (Arthur et al., 2009; King, 2012). The water used in hydraulic fracturing contains chemical and biological additives to prevent scale buildup, prop open the fractures, prevent biological fouling, and generally maximize the extraction of the natural gas (Vidic et al., 2013). A portion of the injected water returns to the surface immediately following hydraulic fracturing; chemical analyses of these flowback waters show large increases in total dissolved solids (salinity and

heavy metal species such as As and Se) likely generated from the interaction between the injection fluid and the black shale (Balaba and Smart, 2012; Gregory et al., 2011; Nicot and Scanlon, 2012; Vidic et al., 2013). Direct observations of the geochemical reactions occurring within the black shale during hydraulic fracturing operations, however, are relatively few, hindered by the depth of the shale formations commonly targeted and the corresponding high pressure, high temperature conditions. Under experimental conditions of high pressure and temperature, Marcon et al. (2017) provided evidence for clay and carbonate dissolution, secondary clay and anhydrite precipitation, and possibly metal adsorption from solution in an experiment reacting synthesized hydraulic fracturing fluid and black shale samples. The objective of this study is to follow up on the work of Marcon et al. (2017) and specifically evaluate the REE behavior during reactions between hydraulic fracturing fluid and black shale. We measured the preserved experimental fluids of Marcon et al. (2017) for the REEs and conducted additional experiments at different pressure, temperature, and initial pH conditions in order to document the impact of these factors upon the dissolved REE system. The results of this study may guide the utility in using REEs as tracers of geochemical reactions with shale and revealed that REEs are not recoverable as a byproduct of hydraulic fracturing of the Marcellus shale.

2. METHODS

2.1 Shale material and location

The black shale samples used in this study are from the Whipkey ST1 Core, which was drilled by the Eastern American Energy Corporation in Greene County, Pennsylvania. We present the dissolved REE contents in the reacted fluids from experiments performed by Marcon et al. (2017), designated as Experiment 1, as well as our corollary experiment at high pressure

and temperature, designated as Experiment 2 (Table 1). Marcon et al. (2017) used samples from 7,846 ft deep in the Whipkey core in Experiment 1 whereas Experiment 2 was sampled from three different depths at 7,801 ft, 7,833 ft, and 7,846 ft in order to generate enough sample volume to run the experiments (Fig. 1). The deepest sample from 7,846 ft is from an organic-rich unit (C_{org} = 5.5 wt%) within the Whipkey Core that is described by Chen and Sharma (2016) as being deposited under alternating redox conditions spanning from suboxic to anoxic on the basis of redox-sensitive trace metal accumulation and elevated C:P ratios. The two samples from 7,801 ft and 7,833 ft are relatively less rich in organic carbon (C_{org} = 2.1 - 2.6 wt%) and were deposited under dominantly suboxic conditions (Chen and Sharma, 2016). The whole-rock REE content of the samples are from Yang et al., (2017) and were determined through a microwave-assisted acid digestion method that uses a mixture of hydrofluoric (HF), nitric (HNO_3), and hydrochloric (HCl) acids heated and pressurized in a microwave vessel to completely dissolve the rock sample.

Table 1: Experiment conditions

	Temperature	Pressure	Fluid	Fluid:rock ratio	Sampling Intervals
	°C	MPa		w:w	hrs
Experiment 1	130	27.5	complex brine	20:1	0, 24, 48, 170, 240, 360
	130	27.5	complex brine+FF	20:1	0, 24, 48, 170, 240, 360
Experiment 2	50	25	brine	20:1	170
	50	25	brine+FF	20:1	170
	50	25	brine+acid	20:1	170
	50	25	brine+FF+acid	20:1	170
	90	27.5	brine	20:1	170
	90	27.5	brine+FF	20:1	170
	90	27.5	brine+acid	20:1	170
	90	27.5	brine+FF+acid	20:1	170

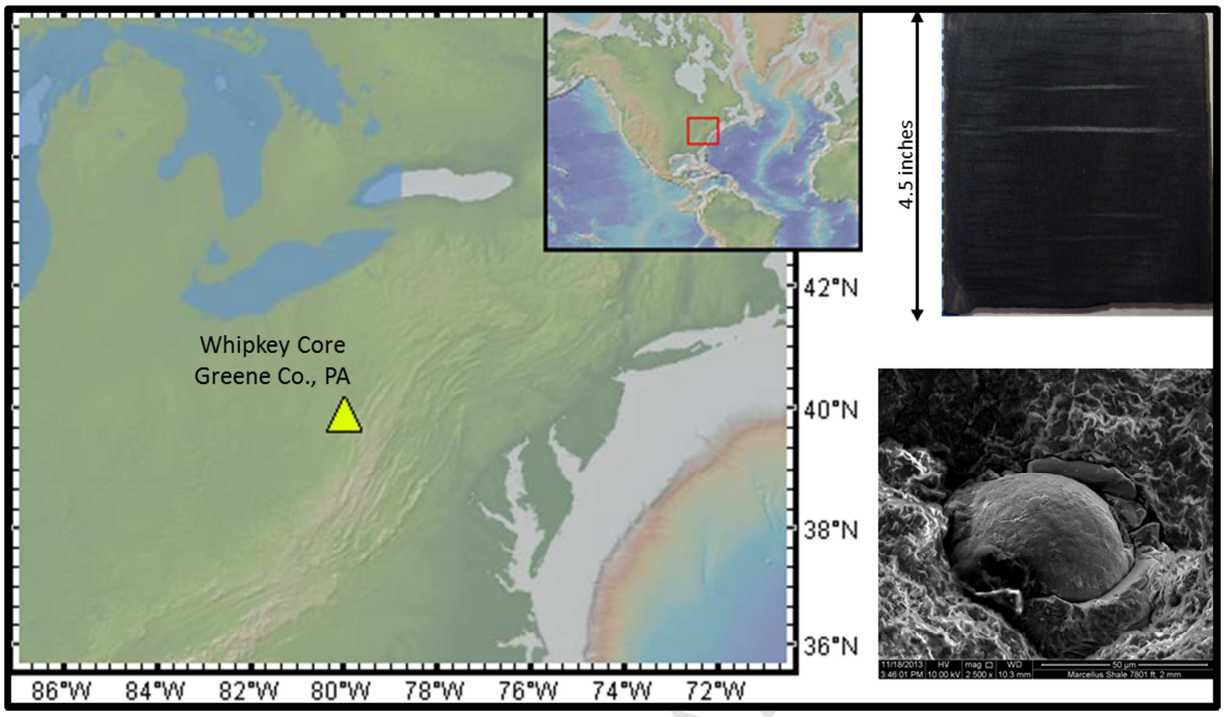

Figure 1: Location of the Whipkey Core, Marcellus Formation in Southwestern Pennsylvania. Upper right hand corner shows a photo of the core sample taken. Bottom right hand corner shows a representative SEM image of the shale

2.2 Experimental design

The high pressure and temperature reactions were conducted in rocking autoclave reactors (Coretest Systems, Inc.) using flexible gold reaction cells and titanium capillary exit tubes following the methods described in Marcon et al. (2017), designed after Kaszuba et al. (2005, 2003) and Seyfried et al. (1987). Briefly, the flexible gold reaction cells provide an inert reaction vessel into which the shale samples and reaction fluids are placed. These gold cells are then sealed and placed in a stainless steel pressure vessel filled with water as the confining fluid. The entire apparatus is mounted within a rocking autoclave body that rocks slowly back and forth through 90 degrees of motion from the upright vertical to horizontal orientations so that there is constant mixing of the shale samples and reaction fluids. Titanium capillary exit tubes mounted to the gold cell body allows fluids to be withdrawn from the reaction vessel while

maintaining pressure and temperature conditions (see Appendix A). Experiment 1 was performed at 27.5 MPa|130 °C for a total duration of 360 hrs and reaction fluids were sampled at time steps of 0, 24, 48, 170, 240, and 360 hrs at experimental pressures and temperature (Table 1). This pressure and temperature regime was selected by Marcon et al. (2017) to approximate bore hole conditions on the Marcellus shale. The temperature was elevated from the actual bore hole temperature of 75 °C to 130 °C to enhance mineral kinetics while maintaining the same mineral thermodynamic profile.

The fluids used in Experiment 1 were a synthetic brine solution prepared based on geochemical modelling of Marcellus formation fluids and a synthesized fracturing fluid (Appendix A). To model the Marcellus formation fluids, Marcon et al. (2017) used the Geochemist's Workbench modelling software to react Marcellus shale with a dilute water at 75 °C and 275 bars (the approximate conditions in the shale formation) until equilibrium was reached. The mineralogy of the Marcellus shale was parameterized based on XRD analyses of the Whipkey Core samples, which showed major components (> 25 %) of quartz and muscovite/illite (Marcon et al., 2017). The general composition of the fracturing fluid is described in Kekacs et al. (2015) and was developed based on information available from fracfocus.org, which is a chemical disclosure registry for hydraulic fracturing fluids (Ground Water Protection Council and The Interstate Oil and Gas Compact Commission, 2017) (Appendix A).

For Experiment 1, two reactors were used: one containing shale and the synthetic brine (as a control), and the other containing shale and a 70:30 (v:v) ratio of synthetic brine to synthetic fracturing fluid (designated as brine+FF) to evaluate effects of fracturing fluid on shale reactions (Marcon et al., 2017). Approximately 25 g of solid shale samples were reacted with ~

500 g of reaction fluids, in a fluid:rock ratio of 20:1. The shale consisted of Whipkey Core shale samples that had been broken down into size fractions of 1 – 3 mm chips and < 147 µm powder in an approximate 3:1 ratio of powder to chips. This ratio was chosen to drive fluid-rock reactions and to provide a surface to analyze dissolution/precipitation reactions (Marcon et al., 2017).

Experiment 2 followed the general framework of Experiment 1, and was also performed in a series of two rocking autoclave reactors. Since Marcon et al. (2017) showed that the majority of the changes in fluid chemistry occurred in the first 24 - 48 hrs of Experiment 1, we ran Experiment 2 for an abbreviated duration of 170 hrs to expedite time windows while still ensuring enough time for reactions to occur at the specified pressures and temperatures (Table 1). Additionally, for Experiment 2 we ran experimental conditions at lower temperatures of 25 MPa|50 °C or 27.5 MPa|90 °C to be consistent with approximate conditions in the bore hole. For each experimental condition, one reactor contained shale and synthetic brine as a control while the other reactor held shale and a 70:30 (v:v) ratio of synthetic brine to synthetic fracturing fluid. Since Experiment 2 was primarily structured as an exploratory study into the potential release of REEs from hydraulically fractured shale, we used a simple NaCl brine (44.5 g/L) rather than the complex brine in Experiment 1 to evaluate whether a signal of released REEs could be detected (Appendix A).

For Experiment 2, acidified and non-acidified conditions, using ultrapure HCl (*Trace*SELECT Ultra from Sigma-Aldrich) to adjust the pH of the acidified solutions to values < 2, were also compared. Pre-reaction fluid samples for Experiment 2 were collected prior to any contact with the rock; initial time fluid samples were collected after the introduction of the rock to the fluid but prior to being brought to high pressure and temperature (t = 0 hrs); and post-

reaction samples were collected after 170 hrs of reaction at high pressure and temperature (t = 170 hrs). The black shale samples used in Experiment 2 were from depths of 7,801, 7,833, and 7,846 ft in the Whipkey Core, homogenized in a mixture of size fractions of 6.4 mm, 2 mm, 1 mm, and < 0.5 mm.

2.3 Analytical Methods

For Experiment 1, dissolved cation concentrations were determined in filtered, nitric acid-preserved samples by ICP-OES (Perkin Elmer DV7300) and ICP-MS (Nexion), and dissolved anion concentrations determined in filtered, non-acidified samples by ion chromatography (Dionex) as reported in Marcon et al., (2017). For Experiment 2, fluid samples were passed through 0.45 µm polysulfone filters and acidified to pH < 2 using ultrapure HCl (*Trace*SELECT Ultra from Sigma-Aldrich) immediately following collection. Major cations (Ba, Ca, Sr, K) for Experiment 2 were measured on a Leeman Teledyne Prodigy ICP-OES at Oregon State University. Detection limits were below 0.3 mg/L for Ca and K and below 0.01 mg/L for Sr and Ba. Reproducibility of the data was typically below 5 - 6 % (1σ) based on triplicate measurements of the samples. The samples in Experiment 2 were then prepared by an acid digestion using 1 M HCl (1x quartz-distilled) and processed through cation exchange columns using 1.8 mL Bio-Rad AG50-X8 (100-200 mesh) resin to isolate the REEs. The resulting eluents were then converted into a 1 % (w/w) HNO_3 (1x quartz-distilled) matrix and analyzed on a Thermo XSeriesII ICP-MS. Detection limits were below 7 µg/L for all the REEs. External reproducibility of the cation columns was assessed through duplicate analyses of an acid mine drainage water PPREE1 from (Verplanck et al., 2001) and found to vary less than 4.5 % (1σ) for all of the REEs except for Tm, which varied by 9 %. The external accuracy of PPREE1 through cation columns was within reported error for REEs in PPREE1 (Verplanck et al., 2001).

3. RESULTS

The total REE content of the three depth intervals (7,801 ft, 7,833 ft, and 7,846 ft) used from the Whipkey Core ranged from 145 - 170 µg/g. A common practice when evaluating the REEs is to normalize the concentrations to average continental shale both to assess the relative differences between the given sample and an average crustal composition and to elucidate the relative changes between the light, middle, and heavy mass REEs in a sample. For these experiments, we normalize REE concentrations to Post-Archean Australian Shale (PAAS) (Taylor and McLennan, 1985). Typical values of REEs in continental shale average approximately 180 µg/g (Taylor and McLennan, 1985). The REE patterns of the three depth intervals from the Whipkey Core show relatively flat, unstructured patterns relative to PAAS (Fig. 2). By comparison, black shales from the Hushpuckney and Stark units are enriched in the REEs with contents ranging from 280 - 380 µg/g with a distinct peak in the middle REEs. Samples from the Woodford Shale, on the other hand, are rather low in REE content, averaging 77 µg/g in an unremarkable, flat pattern. The range of REE content in black shales is highly variable, but the Marcellus Shale samples utilized in this study are an average representation.

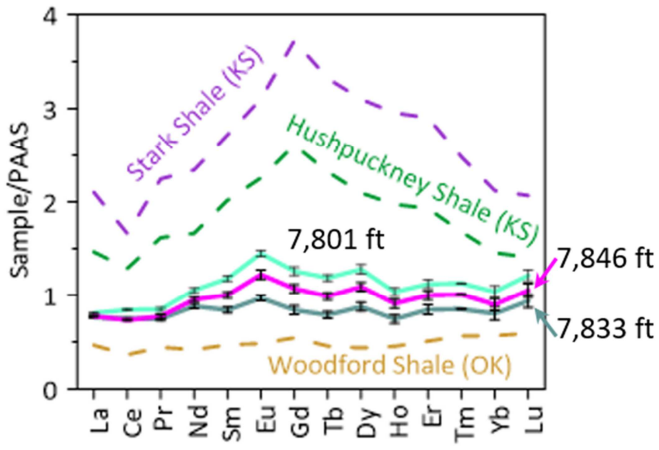

Figure 2: PAAS-normalized REE patterns of the three samples of the Marcellus Shale from the Whipkey Core in southwestern Pennsylvania. Also plotted for comparison are samples from the

Stark and Hushpuckney shales of Kansas and the Woodford shale of Oklahoma (REE data from Yang et al., 2017).

3.1 Dissolved major cations

The dissolved major constituents in the fluids of Experiment 1 are reported and discussed in Marcon et al. (2017) and the salient results are summarized here. Briefly, dissolved Sr and Ba in the reaction fluids increased sharply after the initial contact of the fluids with the shale samples at t = 0 hrs (Fig. 3, 4). Following this initial increase, dissolved Sr and Ca increased more gradually in the brine fluids (Fig. 3) and were relatively constant in the brine+FF fluids (Fig. 4). Dissolved K remained at relatively constant levels, and dissolved Ca was at relatively constant levels in the brine fluids of Experiment 1. In the brine+FF fluids, dissolved Ca increased sharply during the first contact of the fluids with the shale samples and thereafter remained relatively constant for the duration of the experiment.

In contrast to Experiment 1 fluids, the dissolved concentrations of Ca, K, Sr, and Ba are significantly lower in Experiment 2 reaction fluids (Fig. 3, 4). For Experiment 2 reaction fluids, dissolved Ca increased upon the first contact with the shale samples, from below detection limits of 0.2 mg/L up to values of 2 to 12 mg/L. This increase is consistent between the brine and brine+FF fluids as well as between acidified and un-acidified conditions. In the un-acidified brine at 25MPa|50 °C, the increase in dissolved Ca was significantly higher, up to 70 mg/L (Fig. 3). By the conclusion of Experiment 2 after an elapsed time of 170 hrs, dissolved Ca increased further in the reaction fluids to values of 97 to 200 mg/L, with the fluids reacted at 27.5MPa|90 °C generally showing a greater increase. Dissolved K showed similar increases in concentrations from the starting fluid compositions to the introduction of shale samples to the conclusion of the experiment at t = 170 hrs (Fig. 3, 4). For all fluid compositions and temperature and pressure

conditions, dissolved K increased from the first contact between the fluid and shale, increasing from 8.7 - 12.5 mg/L in the starting fluids to 25 - 40 mg/L. After the elapsed reaction time of 170 hrs, K concentrations increased slightly to 34 - 46 mg/L. Dissolved Sr values in the starting fluid compositions were below detection limits (0.003 mg/L) but increased to values of 1.0 - 2.1 mg/L after the reaction at t = 170 hrs (Fig. 3,4). Similar to the observations of dissolved Ca, dissolved Sr showed the greatest increase from below detection limits up to 1.2 mg/L at the introduction of the shale samples to the fluids at t = 0 hrs in the un-acidified brine at 25 MPa|50 °C (Fig. 3). Dissolved Ba concentrations increased from below detection limits of 0.12 mg/L in the starting fluid composition to a value ~ 0.4 mg/L after the introduction of the shale sample to the fluids at t = 0 hrs (Fig. 3,4). After the elapsed time of 170 hrs, the dissolved Ba in the fluids reacted at 25 MPa|50 °C remained at ~ 0.4 mg/L, whereas fluids reacted at 27.5 MPa|90 ° increased to values of 0.8 - 1.3 mg/L.

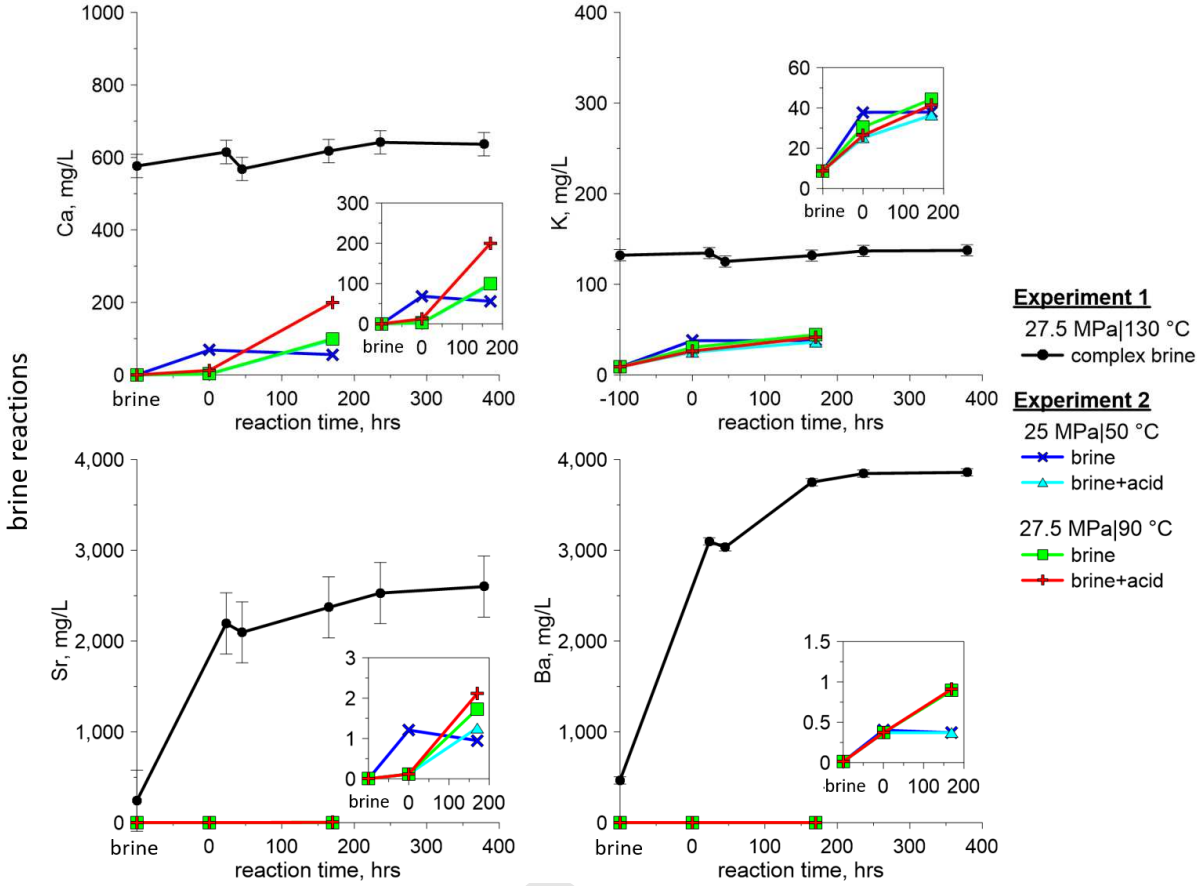

Figure 3: Major dissolved cations (Ca, K, Sr, Ba) for Experiment 1 (Marcon et al., 2017) and Experiment 2 brine fluids over the duration of the experiment. Insets show a closer view of the changes in Experiment 2 fluids. Time points shown on the x-axis begin with the starting fluid composition before contact with the shale. Time point t = 0 hrs represents the onset of the high pressure, high temperature experiments when the fluids are first contacted with the shale. Error bars shown are 1σ standard error. In cases where error bars are not shown, the error is smaller than the size of the symbol used.

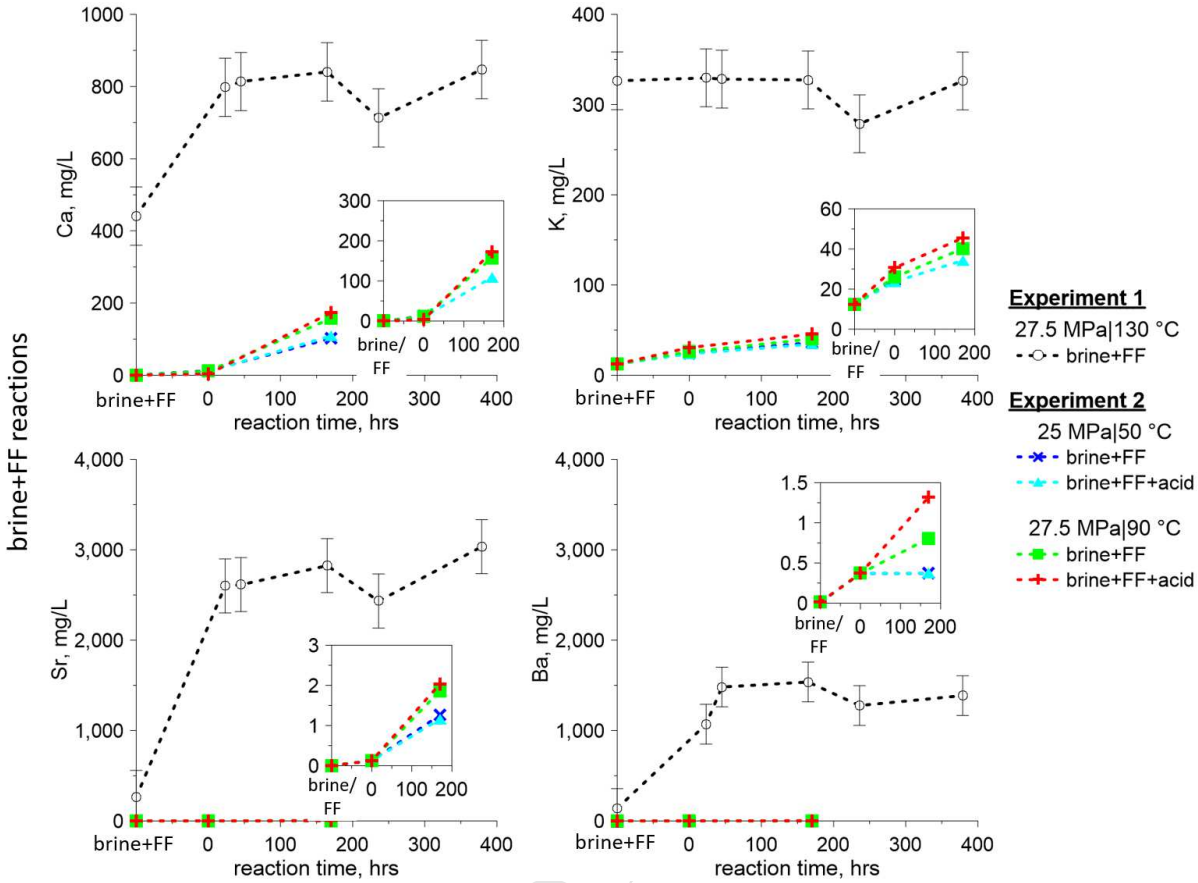

Figure 4: Major dissolved cations (Ca, K, Sr, Ba) for Experiment 1 (Marcon et al., 2017) and Experiment 2 brine and fracturing fluid mixtures over the duration of the experiment. Insets show a closer view of the changes in Experiment 2 fluids. Time points shown on the x-axis begin with the starting fluid composition before contact with the shale. Time point t = 0 hrs represents the onset of the high pressure, high temperature experiments when the fluids are first contacted with the shale. Error bars shown are 1σ standard error. In cases where error bars are not shown, the error is smaller than the size of the symbol used.

3.2 Dissolved REEs over reaction time

Dissolved REEs in the Experiment 1 brine were below the limits of detection (0.009 µg/L) for the entirety of the 360 hour reaction time and thus are omitted from Fig. 5. Similarly, the dissolved REE concentrations of the Experiment 2 brine fluids at the t = 0 hr and t = 170 hr time points were below the limit of detection and also omitted. Here we show the dissolved REE concentrations as the sum of all 14 REEs to highlight the main trends of the series for the

duration of the reactions. The starting composition of the brine fluids in Experiment 2 contained an average of 15.4 µg/L of total REEs (Fig. 5). In the acidified brine fluids, the total REE content increased to 17.3 µg/L for the 25 MPa|50 °C reaction and to 16.5 µg/L for the 27.5 MPa|90 °C reaction at time point t = 0 hrs, when the shale samples were first introduced to the fluids. After the elapsed reaction time of 170 hrs for Experiment 2, the REE content in the acidified brine fluids decreased slightly to 17.0 µL for the 25 MPa|50 °C reaction and to 15.3 µg/L for the 27.5 MPa|90 °C reaction. We do note, however, that these average total REE concentrations in the acidified brine fluids of Experiment 2 are within reported error (1σ) of each other and differences between the time points are thus likely minimal (Fig. 5).

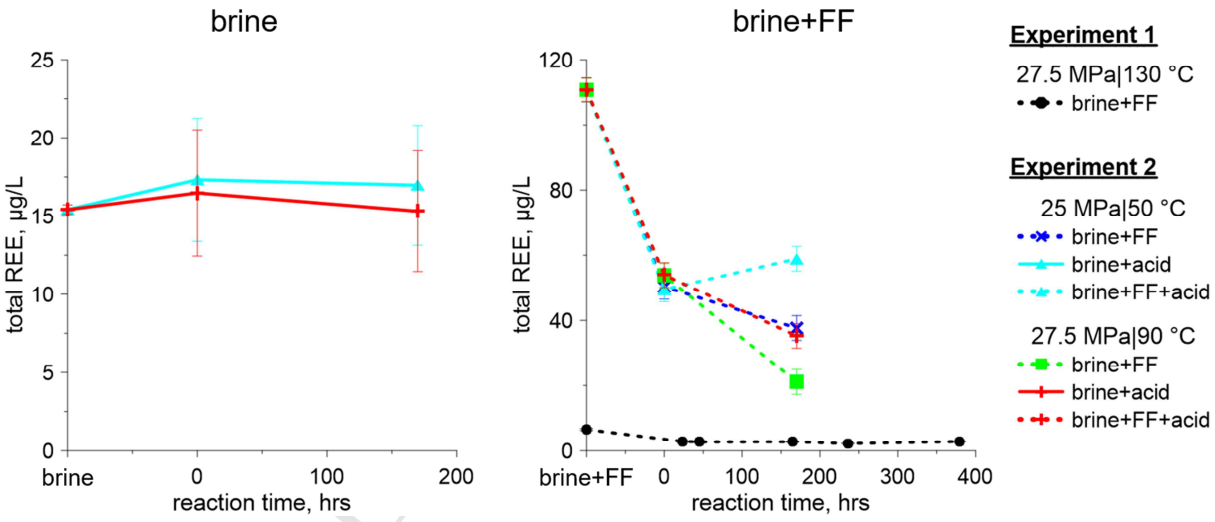

Figure 5: Concentrations (µg/L) of total dissolved REEs in Experiment 1 and Experiment 2 fluids sampled at discrete time intervals for the 360 hour total duration of the reaction. Note the scale on the y-axis. The panel on the left shows the reaction of the brine fluids. The panel on the right shows the reaction of the brine/fracturing fluid mixture.

The starting composition of the brine+FF fluids in Experiment 1 contained an average of 6.4 µg/L of total REEs (Fig. 5). By time point t = 24 hrs, the total dissolved REE content in the Experiment 1 brine+FF fluids had decreased by more than half to 2.8 µg/L. For the remainder of the reaction time, the total dissolved REE content remained relatively constant, varying no more

than 3% from an average of 2.75 µg/L, except at t = 240 hrs which had a lower REE content of 2.2 µg/L. The starting composition of the brine+FF fluids in Experiment 2, by comparison, contained an average of 110 µg/L total REEs (Fig. 5). After the introduction of the shale samples at time point t = 0 hrs, the total REE content decreased to 49.5 - 53.9 µg/L in all of the brine+FF fluids of Experiment 2. After the total reaction time of 170 hrs, the total REEs decreased further to 21.0 - 37.6 µg/L, except for the acidified brine+FF fluid at 25 MPa|50 °C, where the total REE content increased to 58.9 µg/L at t = 170 hrs (Fig. 5). These changes in concentrations of the dissolved REEs, however, are still three orders of magnitude less than the concentrations of REEs reported in the solid shale samples.

In addition to the main trends identified in the total REE contents of the reaction fluids, we also evaluate the relative differences and changes between the individual REEs by normalizing the dissolved REE concentrations to PAAS (Fig. 6, 7). In Experiment 1 brine+FF fluids, after the initial decrease in total REE concentrations within the first 24 hrs, the total REE concentrations remain relatively constant for the remainder of the reaction and are reflected in PAAS-normalized patterns that are indistinguishable between the various time points (Fig. 6). These patterns are characterized by a depletion in the light REEs (La, Ce, Pr, Nd) relative to the starting composition and a linear enrichment in the middle (Sm, Eu, Gd, Tb, Dy) and the heavy (Ho, Er, Tm, Yb, Lu) REEs.

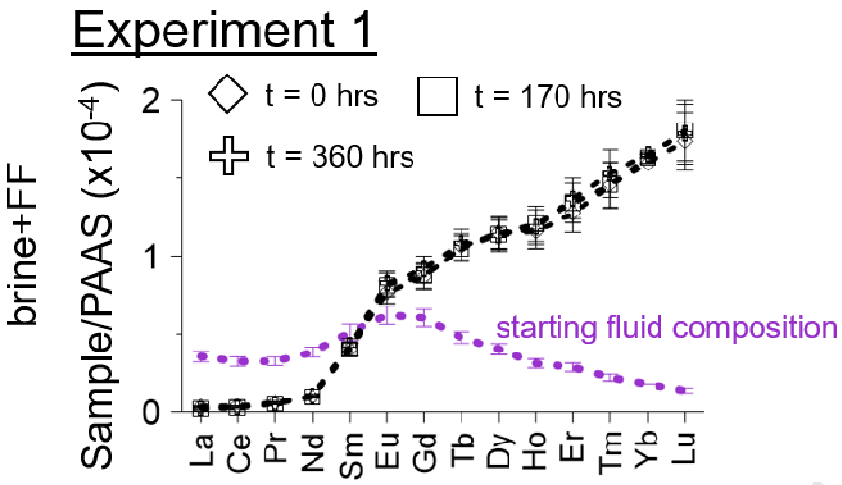

Figure 6: PAAS-Normalized REE patterns of the brine+FF fluids in Experiment 1. The starting composition of the brine+FF fluids are shown in purple. Time points at t = 0 hrs (open diamonds), t = 170 hrs (open squares), and t = 360 hrs (open crosses) are shown for comparison. For the brine+FF fluids in Experiment 1, no change in total REE content from time point t = 0 hrs to the end of the reaction was discernible and the three selected time points plot together.

In Experiment 2 fluids, the REE patterns were largely similar throughout the course of the reaction in terms of the overall distribution and shape of the pattern (Fig. 7). The starting composition of the brine fluids had a relatively flat REE pattern, but did exhibit a small peak in the middle REEs centered on Gd. In the brine fluids of Experiment 2, the dissolved REEs fell below the detection limits at time points t = 0 hrs and t = 170 hrs and are thus omitted from Fig. 7. In the acidified brine solutions, where we observed a slight increase in total REE concentrations at t = 0 hrs (open diamonds) followed by a slight decrease at t = 170hrs (open squares), we observe from the PAAS-normalized patterns that these changes may be attributable to slight increases in the middle and heavy REEs, particularly under the 25 MPa|50 °C conditions (Fig. 7). As noted in the total REE concentration profile, however, these changes are relatively minor within the reported error range and the REE patterns are similar in magnitude and shape to the starting fluid composition. The starting composition of the brine+FF fluids in Experiment 2 is characterized by a strong peak in the middle REEs centered on Eu (Fig. 7). At t = 0 hrs (open

303 diamonds), the magnitude of the REE patterns decreased while retaining a middle REE peak,
304 corresponding to the decreases observed in the total dissolved REE profiles. At t = 170 hrs (open
305 squares), the REE patterns decreased by a lesser amount, again reflecting the slight decreases in
306 total dissolved REE concentrations, except for the acidified brine+FF fluid under 25 MPa|50 °C
307 conditions, which increased in magnitude. Consistent throughout all of the time points for the
308 brine+FF fluids of experiment 2, however, was a pattern characterized by a middle REE peak.

309

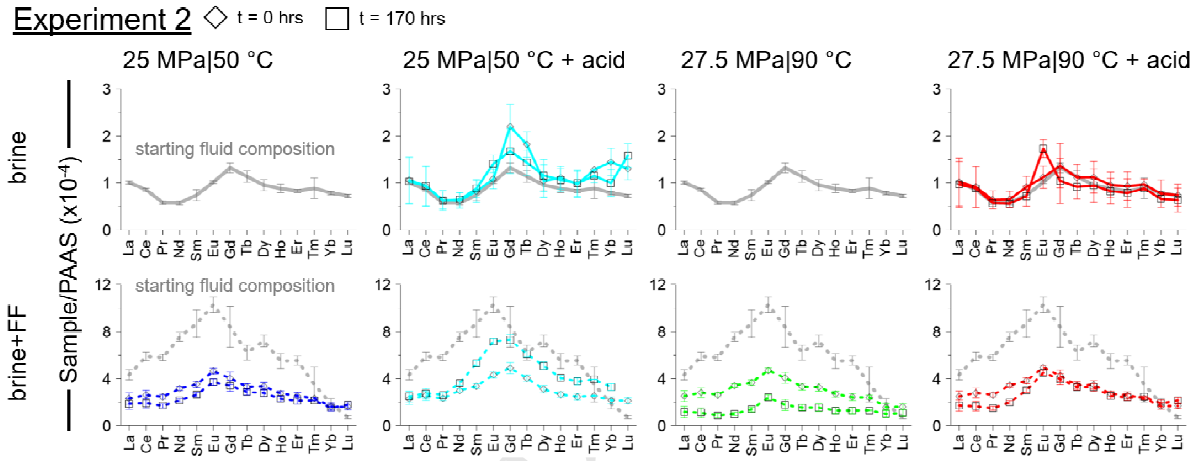

310 Figure 7: PAAS-Normalized patterns of the dissolved REEs in Experiment 2 fluids. The starting
311 fluid composition of the brine (top row) and brine+FF fluids (bottom row) are shown for
312 comparison. Results from time point t = 0 hrs are denoted by open diamonds. Results from time
313 point t = 170 hrs are denoted by open squares. Dissolved REEs in the un-acidified brine fluids at
314 t = 0 hrs and t = 170 hrs were below the limit of detection and thus omitted.

315 4. DISCUSSION

316 The results of these high pressure, high temperature experiments on the Whipkey Core
317 (Marcellus shale) demonstrate that the REEs were not mobilized to any significant extent (> 1.8
318 µg/L) from the solid shale phase into the fluid phase during simulated down-hole conditions that
319 approximate conditions of hydraulic fracturing operations. These results are independent of the
320 time of reaction, the initial pH of the solution, or the composition of the fluid used in these

321 particular experiments. Rather than a net mobility of REEs from solid to fluid phase, the results
322 of Experiment 1 and 2 indicate a net loss of REEs from the fluid phase.

323 For these simulated hydraulic fracturing systems, Marcon et al. (2017) documented
324 evidence for carbonate and pyrite dissolution through the proportional release of dissolved Sr,
325 Mn, Mg, Fe, SO_4, Ba, and Ca to the fluids in Experiment 1 (Fig. 3, 4). A similar expression of
326 these dissolved species in the fluids of Experiment 2 is also observed although at much lower
327 concentrations that could reflect sample heterogeneities and differences between the size
328 fractions of shale sample used. Sample heterogeneity between these autoclave systems could also
329 potentially account for the recorded increase of REEs in the one acidified brine+FF fluid at 25
330 MPa|50 °C. Despite these potential heterogeneities between shale samples, the occurrence of
331 carbonate dissolution is likely for both Experiments 1 and 2. Carbonates play an important role
332 as a potential sink of the REEs in marine sediments. Carbonate formation at cold seep locations
333 in the marine environment has been shown to very efficiently scavenge the REEs from the
334 interstitial pore waters in the sediments (Bayon et al., 2007; Himmler et al., 2010; Rongemaille
335 et al., 2011; Zhong and Mucci, 1995). The subsequent dissolution of carbonates in black shale
336 formations when accessed by hydraulic fracturing fluids, thus, might be expected to release these
337 REEs into solution. The lack thereof of a signal in the dissolved REE concentrations from this
338 carbonate dissolution suggests that: 1) there was a lack of REEs in the carbonate phase of the
339 black shale samples used; or 2) there was a strong removal process of dissolved REEs from the
340 fluid phase.

341 The shale samples under reaction with these fluids are relatively low in carbonate content
342 (2 - 4 wt%) and have furthermore been recently shown to host the REEs dominantly in remnant
343 organic matter and siliciclastic materials rather than more accessible carbonate minerals (Yang et

al., 2017). In the carbonate fraction of these black shale intervals isolated through a Na-acetate extraction, the REEs have been measured in concentrations of 10 - 20 µg/g whole rock, accounting for just 6.5 – 10% of the total whole-rock REE content (Yang et al., 2017). Despite this low percentage of REEs found in the carbonate fraction, the dissolution of even a portion of the total carbonate content would be expected to release a measurable signal of dissolved REEs to the fluid phase. For example, taking the Experiment 2 results as a basis, if we assume that the increases in dissolved Ca concentrations in the fluids are from the dissolution of carbonate minerals, then over the course of the reaction a total increase of ~ 50 - 100 mg/L in dissolved Ca is attributable to carbonate dissolution (Fig. 3, 4). These increases roughly correspond to the dissolution of ~ 5 – 10 % of the total carbonate (as $CaCO_3$) present in the shale samples, which is measured at 2 - 4 wt% in the bulk shale material. A 5 - 10 % release of the REEs bound in the carbonate fraction to the fluid phase would result in increases in dissolved REE concentrations of ~ 25 - 100 µg/L, which is not observed in the corresponding fluid data.

Another aspect to carbonate dissolution that is relevant to REE chemistry is the formation of dissolved REE-carbonate complexes in solution, where the complexation of dissolved REEs with dissolved carbonate (and other dissolved species such as silica and organic ligands) retains the REEs in solution (e.g., Akagi, 2013; Byrne and Li, 1995; Cantrell and Byrne, 1987; Pourret et al., 2007). The formation of these dissolved complexes are favored strongest for the heavy REEs and less favored towards the light REEs, and may be observed in the fluid phase as a relative enrichment of the heavy REEs to the light REEs relative to a reference standard such as PAAS. We observe a heavy REE enriched pattern in the Experiment 1 brine+FF fluids that may suggest that complexation plays a small role in this system, although the total magnitude of dissolved REE concentrations is small relative to the expected release of REEs from carbonate

dissolution as discussed above (Fig. 6). In the Experiment 2 fluids, no such heavy REE enriched patterns are observed, with the dissolved REE concentrations being quantitatively removed instead (Fig. 7). Despite evidence for carbonate dissolution and alteration, the lack of a corresponding increase in the dissolved REE concentrations suggests that other processes are exerting a stronger influence on the REEs in these simulated systems.

In Experiments 1 and 2, the minimal expression, and even net loss, of the REEs in the fluids suggests that rather than mobilization of the REEs from these Marcellus Shale samples there is a strong removal term that is likely either surface adsorption or incorporation into precipitating mineral phases. In dissolved seawater, for example, the REEs show a strong propensity for surface adsorption onto marine particles, where adsorption constants are greatest for the light REEs and decrease towards the heavy REEs (Alibo and Nozaki, 1999; Byrne and Li, 1995; Koeppenkastrop and De Carlo, 1992; Sholkovitz et al., 1994). By contrast, in ground water studies, the solution complexation of the REEs has been shown to exert a greater influence on the REE system than surface adsorption (Johannesson et al., 1997a, 1997b; Worrall and Pearson, 2001). The complexation and adsorption behavior of the REEs is strongly dependent on the pH and alkalinity of the fluids (e.g., Bau et al., 1996; Byrne and Li, 1995; Sholkovitz, 1995). In acidic waters (pH < 3.5), the dissolved REEs are present dominantly as free metal species (Ln^{3+}, where Ln is any of the REEs) (e.g., Johannesson et al., 1996a). In higher pH waters, REE-carbonate complexes are the dominant species in solution (e.g., Cantrell and Byrne, 1987; Johannesson et al., 1996b). Simultaneously, however, with increasing pH, adsorption of the REEs onto particle surfaces increases (e.g., Sholkovitz, 1995). In our Experiment 1 and 2 fluids, the dissolution of carbonate likely buffered the fluids to higher pH levels over the course of the reaction as well as provided dissolved carbonate species for complexation. Despite this increased

availability of dissolved carbonate species to potentially complex the REEs in solution, the corresponding increase in pH likely favored the adsorption of the REEs onto the shale particle surfaces. The adsorption of REEs onto particle surfaces would be consistent with the net loss of REEs observed in the Experiment 1 and 2 fluids. Interestingly, the acidified brines of Experiment 2 were the only fluids where a net decrease in the dissolved REEs was not observed (Fig. 7). Although these fluids were initially adjusted to a pH below 2, this pH was not maintained throughout the duration of the experiment and evidence for carbonate dissolution likely indicate that pH levels increased, although pH was not monitored. In Experiment 1, however, Marcon et al. (2017) found that the more acidic brine+FF fluids recorded an increase in pH to values of ~ 5.5, which was slightly lower than the pH increase to ~ 6 for the brine fluids. We suggest that a similar process may have occurred in the acidified brines of Experiment 2 and that this slightly lower pH value may have been sufficient to maintain these low dissolved REE levels.

Another possibility to the fate of dissolved REEs in these systems is their incorporation into secondary clay minerals such as nontronite, anhydrite, or barite minerals that precipitate from the fluids. From Experiment 1 fluids, Marcon et al. (2017) found evidence for the formation of these mineral phases in modelled saturation indices in the fluid, as well as direct observations of anhydrite formation in the recovered solid samples. The formation of such phases likely entraps the REEs from solution since the precipitation of mineral phases is well-known to very efficiently scavenge and sequester the REEs from the pore waters of marine sediments (e.g., Bright et al., 2009; Feng et al., 2009; Himmler et al., 2010; Rongemaille et al., 2011). Similarly, for hydraulic fracturing fluids, the precipitation or alteration of mineral phases provides a likely mechanism for REE removal from solution. For our particular experiments, the capacity of precipitating phases to sequester the REEs was not directly quantified owing to the challenges in

413 measuring small quantities of REEs within precipitate phases that are themselves present only in
414 small amounts (Marcon et al., 2017).

415 The limited expression of the REEs to the fluid phase during water-rock interactions in
416 hydraulic fracturing holds potential implications to their applicability as geochemical tracers of
417 hydraulic fracturing processes and is consistent with other systems such as Sr isotopes that are
418 being used to characterize and trace produced waters on the Marcellus Shale (Capo et al., 2014;
419 Chapman et al., 2012; Kolesar Kohl et al., 2014). These Sr isotopes within produced waters
420 revealed that the signal of Sr from geochemical reactions between the shale formation and
421 hydraulic fracturing fluid was minor compared to the influence of naturally occurring formation
422 fluids mixing with fracturing fluids (Capo et al., 2014; Chapman et al., 2012; Kolesar Kohl et al.,
423 2014). Similarly, the REEs may exhibit a similar behavior, where the water-rock interactions
424 between the shale formation and the hydraulic fracturing fluid may only play a minor role in the
425 cycling of these trace element systems, affecting our ability to apply the REEs as a geochemical
426 tracer of hydraulic fracturing operations.

427 This conclusion on REE mobility in hydraulically fractured systems, however, must be
428 applied with caution, as considerable variability exists within black shale systems targeted for
429 hydraulic fracturing and within the fracturing fluids themselves. Certainly within the conditions
430 imposed on Experiments 1 and 2, REE mobility from the Marcellus shale into solution is limited,
431 thus implying the inappropriateness of using the REEs as geochemical tracers and the
432 improbability of the REEs being a byproduct of hydraulic fracturing. The black shale samples
433 from the Marcellus Shale, though, did not contain an appreciable amount of REEs within an
434 accessible carbonate or authigenic phase to begin with and furthermore contained only an
435 average amount (~ 185 µg/g) of REEs within the whole-rock sample. Comparatively, black shale

sequences with authigenic phosphorus accumulations can be enriched in the REEs up to ~ 700 µg/g in the whole-rock composition (Chen and Sharma, 2016; Yang et al., 2017; Zhang et al., 2016). REE concentrations within sedimentary phosphorous deposits additionally may range up to 5,000 µg/g (e.g., Emsbo et al., 2015). Given this dynamic variability in REE content amongst black shale units, black shales with a higher REE content, and/or a higher percentage of REEs within carbonate facies, may be more susceptible to release REEs under hydraulic fracturing conditions (Fig. 1). The composition of the hydraulic fracturing fluid is also subject to wide variations on a case to case basis, and while the synthetic fluid used in this study was based on average reported compositions, specific compositions used can vary significantly based on the operator and target formation (e.g., Kekacs et al., 2015). Additional research to evaluate REE mobility in other hydraulically fractured systems is warranted to better understand the utility of REEs as tracers for subsurface fluid-rock reactions.

5. CONCLUSION

The mobility of REEs from the Whipkey Core (Marcellus Formation) black shale into the reacting fluids was negligible and is consistent across the various reaction parameters (e.g. pH, pressure, and temperature). The lack of an observable release of the dissolved REEs from the shale into the fluid is also consistent with recent data showing that REEs are not hosted in appreciable quantities within accessible carbonate phases of the Marcellus Shale. While there was no appreciable release of REEs into the reacting fluids, we did document a net removal term of the REEs that is likely attributable to surface adsorption or incorporation into precipitating mineral phases, although direct quantification of the REE in such mineral phases remains an analytical challenge. Considerable variation exists within hydraulic fracturing plays and the lack of a REE signal from simulated hydraulic fracturing conditions in this study should be

459 considered as a single data point in constraining a wide range of hydraulically fractured systems.
460 The Marcellus Shale is relatively average in the total REE content and hosts the majority of the
461 REEs within inaccessible, refractory phases; other gas-bearing shales with a greater influence
462 from carbonate and reactive phases may prove to display a more active REE cycle. Further work
463 and/or different approaches should be considered in regards to REE mobility from black shales,
464 their subsequent use as geochemical tracers of water/rock interactions in these systems, and the
465 potential recoverability of the REEs for economic gain.

466 6. ACKNOWLEDGEMENTS

467 This work was performed as part of the Energy Policy Act 2005 Complementary Program, U.S.
468 Department of Energy's Office of Fossil Energy. The authors wish to thank Paula Mouser (Ohio
469 State University) who provided the synthetic fracturing fluid used in the experiments and Jaime
470 Toro (West Virginia University) who provided access to the Marcellus Shale samples from the
471 Whipkey Core. Jeffrey Oberfoell (AECOM) and Yvan Alleau (OSU) provided assistance with
472 the autoclave experiments. Data sets associated with this manuscript will be publicly-available
473 through NETL's Energy Data Exchange (edx.netl.doe.gov).

7. REFERENCES

Akagi, T., 2013. Rare earth element (REE)-silicic acid complexes in seawater to explain the incorporation of REEs in opal and the "leftover" REEs in surface water: New interpretation of dissolved REE distribution profiles. Geochim. Cosmochim. Acta 113, 174–192. doi:10.1016/j.gca.2013.03.014

Alexander, T., Boyer, C., Clark George Waters, B., Jochen, V., Le Calvez Houston, J., Rick Lewis Camron Miller Dallas, T.K., John Thaeler, T., Toelle, B.E., Bentley, D., Friend, D., Hresko, J., Mitchell, R., Sylvester, B., Thomson, S., 2011. Shale Gas Revolution. Oilf. Rev. 23, 40–55.

Alibo, D.S., Nozaki, Y., 1999. Rare earth elements in seawater: Particle association, shale-normalization, and Ce oxidation. Geochim. Cosmochim. Acta 63, 363–372. doi:10.1016/S0016-7037(98)00279-8

Alonso, E., Sherman, A.M., Wallington, T.J., Everson, M.P., Field, F.R., Roth, R., Kirchain, R.E., 2012. Evaluating Rare Earth Element Availability: A Case with Revolutionary Demand from Clean Technologies. Environ. Sci. Technol. 46, 3406–3414. doi:10.1021/es203518d

Arthur, J.D., Bohm, B.K., Coughlin, B.J., Layne, M.A., Cornue, D., 2009. Evaluating the Environmental Implications of Hydraulic Fracturing in Shale Gas Reservoirs, in: SPE Americas E&P Environmental and Safety Conference. Society of Petroleum Engineers. doi:10.2118/121038-MS

Balaba, R.S., Smart, R.B., 2012. Total arsenic and selenium analysis in Marcellus shale, high-salinity water, and hydrofracture flowback wastewater. Chemosphere 89, 1437–1442. doi:10.1016/j.chemosphere.2012.06.014

Bau, M., Koschinsky, A., Dulski, P., Hein, J.R., 1996. Comparison of the partitioning behaviours of yttrium, rare earth elements, and titanium between hydrogenetic marine ferromanganese crusts and seawater. Geochim. Cosmochim. Acta 60, 1709–1725. doi:10.1016/0016-7037(96)00063-4

Bayon, G., Pierre, C., Etoubleau, J., Voisset, M., Cauquil, E., Marsset, T., Sultan, N., Le Drezen, E., Fouquet, Y., 2007. Sr/Ca and Mg/Ca ratios in Niger Delta sediments: Implications for authigenic carbonate genesis in cold seep environments. Mar. Geol. 241, 93–109. doi:10.1016/j.margeo.2007.03.007

Bright, C.A., Cruse, A.M., Lyons, T.W., MacLeod, K.G., Glascock, M.D., Ethington, R.L., 2009. Seawater rare-earth element patterns preserved in apatite of Pennsylvanian conodonts? Geochim. Cosmochim. Acta 73, 1609–1624. doi:10.1016/j.gca.2008.12.014

Byrne, R.H., Li, B., 1995. Comparative complexation behavior of the rare earths. Geochim. Cosmochim. Acta 59, 4575–4589. doi:10.1016/0016-7037(95)00303-7

Cantrell, K.J., Byrne, R.H., 1987. Rare earth element complexation by carbonate and oxalate ions. Geochim. Cosmochim. Acta 51, 597–605. doi:10.1016/0016-7037(87)90072-X

Capo, R.C., Stewart, B.W., Rowan, E.L., Kolesar Kohl, C.A., Wall, A.J., Chapman, E.C., Hammack, R.W., Schroeder, K.T., 2014. The strontium isotopic evolution of Marcellus Formation produced waters, southwestern Pennsylvania. Int. J. Coal Geol. 126, 57–63. doi:10.1016/j.coal.2013.12.010

Chapman, E.C., Capo, R.C., Stewart, B.W., Kirby, C.S., Hammack, R.W., Schroeder, K.T., Edenborn, H.M., 2012. Geochemical and Strontium Isotope Characterization of Produced Waters from Marcellus Shale Natural Gas Extraction. Environ. Sci. Technol. 46, 3545–

3553. doi:10.1021/es204005g
Chen, R., Sharma, S., 2016. Role of alternating redox conditions in the formation of organic-rich interval in the Middle Devonian Marcellus Shale, Appalachian Basin, USA. Palaeogeogr. Palaeoclimatol. Palaeoecol. 446, 85–97. doi:10.1016/j.palaeo.2016.01.016
Emsbo, P., McLaughlin, P.I., Breit, G.N., du Bray, E.A., Koenig, A.E., 2015. Rare earth elements in sedimentary phosphate deposits: Solution to the global REE crisis? Gondwana Res. 27, 776–785. doi:10.1016/j.gr.2014.10.008
Engelder, T., 2009. Marcellus 2008: Report Card on the Breakout Year for Gas Production in the Appalachian Basin. Fort Worth Basin Oil Gas Mag. 18–22.
Feng, D., Chen, D., Rn Peckmann, J., Bohrmann, G., 2009. Authigenic carbonates from methane seeps of the northern Congo fan: Microbial formation mechanism. Mar. Pet. Geol. 27, 748–756. doi:10.1016/j.marpetgeo.2009.08.006
Gregory, K.B., Vidic, R.D., Dzombak, D.A., 2011. Water Management Challenges Associated with the Production of Shale Gas by Hydraulic Fracturing. Elements 7.
Ground Water Protection Council, The Interstate Oil and Gas Compact Commission, 2017. FracFocus Chemical Disclosure Registry [WWW Document]. URL http://fracfocus.org/ (accessed 7.25.17).
Himmler, T., Bach, W., Bohrmann, G., Peckmann, J., 2010. Rare earth elements in authigenic methane-seep carbonates as tracers for fluid composition during early diagenesis. Chem. Geol. 277, 126–136. doi:10.1016/j.chemgeo.2010.07.015
Johannesson, K.H., Lyons, W.B., Yelken, M.A., Gaudette, H.E., Stetzenbach, K.J., 1996a. Geochemistry of the rare-earth elements in hypersaline and dilute acidic natural terrestrial waters: Complexation behavior and middle rare-earth element enrichments. Chem. Geol. 133, 125–144. doi:10.1016/S0009-2541(96)00072-1
Johannesson, K.H., Stetzenbach, K.J., Hodge, V.F., 1997a. Rare earth elements as geochemical tracers of regional groundwater mixing. Geochim. Cosmochim. Acta 61, 3605–3618. doi:10.1016/S0016-7037(97)00177-4
Johannesson, K.H., Stetzenbach, K.J., Hodge, V.F., Berry Lyons, W., 1996b. Rare earth element complexation behavior in circumneutral pH groundwaters: Assessing the role of carbonate and phosphate ions. Earth Planet. Sci. Lett. 139, 305–319. doi:10.1016/0012-821X(96)00016-7
Johannesson, K.H., Stetzenbach, K.J., Hodge, V.F., Kreamer, D.K., Zhou, X., 1997b. Delineation of groundwater flow systems in the southern great basin using aqueous rare earth element distributions. Groundwater 35, 8.
Kargbo, D.M., Wilhelm, R.G., Campbell, D.J., 2010. Natural Gas Plays in the Marcellus Shale : Challenges and Potential Opportunities. Environ. Sci. Technol. 44, 5679–5684.
Kaszuba, J.P., Janecky, D.R., Snow, M.G., 2005. Experimental evaluation of mixed fluid reactions between supercritical carbon dioxide and NaCl brine: Relevance to the integrity of a geologic carbon repository. Chem. Geol. 217, 277–293. doi:10.1016/j.chemgeo.2004.12.014
Kaszuba, J.P., Janecky, D.R., Snow, M.G., 2003. Carbon dioxide reaction processes in a model brine aquifer at 200 °C and 200 bars: implications for geologic sequestration of carbon. Appl. Geochemistry 18, 1065–1080. doi:10.1016/S0883-2927(02)00239-1
Kekacs, D., Drollette, B.D., Brooker, M., Plata, D.L., Mouser, P.J., 2015. Aerobic biodegradation of organic compounds in hydraulic fracturing fluids. Biodegradation 26, 271–287. doi:10.1007/s10532-015-9733-6

King, G.E., 2012. Hydraulic Fracturing 101: What Every Representative, Environmentalist, Regulator, Reporter, Investor, University Researcher, Neighbor and Engineer Should Know About Estimating Frac Risk and Improving Frac Performance in Unconventional Gas and Oil Wells. Soc. Pet. Eng. 6–8.

Koeppenkastrop, D., De Carlo, E.H., 1992. Sorption of rare-earth elements from seawater onto synthetic mineral particles: An experimental approach. Chem. Geol. 95, 251–263. doi:10.1016/0009-2541(92)90015-W

Kolesar Kohl, C.A., Capo, R.C., Stewart, B.W., Wall, A.J., Schroeder, K.T., Hammack, R.W., Guthrie, G.D., 2014. Strontium Isotopes Test Long-Term Zonal Isolation of Injected and Marcellus Formation Water after Hydraulic Fracturing. Environ. Sci. Technol. 48, 9867–9873. doi:10.1021/es501099k

Long, K.R., Van Gosen, B.S., Foley, N.K., Cordier, D., 2012. The Principal Rare Earth Elements Deposits of the United States: A Summary of Domestic Deposits and a Global Perspective, in: Non-Renewable Resource Issues. Springer Netherlands, Dordrecht, pp. 131–155. doi:10.1007/978-90-481-8679-2_7

Marcon, V., Joseph, C., Carter, K., Hedges, S., Lopano, C., Guthrie, G.D., Hakala, J.A., 2017. Experimental insights into geochemical changes in hydraulically fractured Marcellus Shale. Appl. Geochemistry 76, 36–50. doi:10.1016/j.apgeochem.2016.11.005

McCarthy, K., Rojas, K., Niemann, M., Palmowski, D., Peters, K., Stankiewicz, A., 2011. Basic Petroleum Geochemistry for Source Rock Evaluation. Oilf. Rev. 23, 32–43.

Nicot, J.-P., Scanlon, B.R., 2012. Water Use for Shale-Gas Production in Texas, U.S. Environ. Sci. Technol. 46, 3580–3586. doi:10.1021/es204602t

Pourret, O., Davranche, M., Gruau, G., Dia, A., 2007. Competition between humic acid and carbonates for rare earth elements complexation. J. Colloid Interface Sci. 305, 25–31. doi:10.1016/j.jcis.2006.09.020

Rongemaille, E., Bayon, G., Pierre, C., Bollinger, C., Chu, N.C., Fouquet, Y., Riboulot, V., Voisset, M., 2011. Rare earth elements in cold seep carbonates from the Niger delta. Chem. Geol. 286, 196–206. doi:10.1016/j.chemgeo.2011.05.001

Seyfried, W., Janecky, D., Berndt, M., 1987. Rocking autoclaves for hydrothermal experiments II: The flexible reaction-cell system, in: Ulmer, G., Barnes, H. (Eds.), Hydrothermal Experimental Techniques. John Wiley & Sons, New York, pp. 216–239.

Sholkovitz, E.R., 1995. The aquatic chemistry of rare earth elements in rivers and estuaries. Aquat. Geochemistry 1, 1–34. doi:10.1007/BF01025229

Sholkovitz, E.R., Landing, W.M., Lewis, B.L., 1994. Ocean particle chemistry: The fractionation of rare earth elements between suspended particles and seawater. Geochim. Cosmochim. Acta 58, 1567–1579. doi:10.1016/0016-7037(94)90559-2

Taylor, S.R., McLennan, S.M., 1985. The continental crust: Its composition and evolution. Blackwell Scientific Pub.,Palo Alto, CA, Palo Alto, CA.

Verplanck, P.L., Antweiler, R.C., Nordstrom, D.K., Taylor, H.E., 2001. Standard reference water samples for rare earth element determinations. Appl. Geochemistry 16, 231–244. doi:10.1016/S0883-2927(00)00030-5

Vidic, R.D., Brantley, S.L., Vandenbossche, J.M., Yoxtheimer, D., Abad, J.D., 2013. Impact of Shale Gas Development on Regional Water Quality. Science (80-.). 340, 1235009–1235009. doi:10.1126/science.1235009

Worrall, F., Pearson, D.., 2001. Water-rock interaction in an acidic mine discharge as indicated by rare earth element patterns. Geochim. Cosmochim. Acta 65, 3027–3040.

621 doi:10.1016/S0016-7037(01)00662-7
622 Yang, J., Torres, M., McManus, J., Algeo, T.J., Hakala, J.A., Verba, C., 2017. Controls on rare
623 earth element distributions in ancient organic-rich sedimentary sequences : Role of post-
624 depositional diagenesis of phosphorus phases. Chem. Geol. 0–1.
625 doi:10.1016/j.chemgeo.2017.07.003
626 Zhang, L., Algeo, T.J., Cao, L., Zhao, L., Chen, Z.-Q., Li, Z., 2016. Diagenetic uptake of rare
627 earth elements by conodont apatite. Palaeogeogr. Palaeoclimatol. Palaeoecol. 458, 176–197.
628 doi:10.1016/j.palaeo.2015.10.049
629 Zhong, S., Mucci, A., 1995. Partitioning of rare earth elements (REEs) between calcite and
630 seawater solutions at 25°C and 1 atm, and high dissolved REE concentrations. Geochim.
631 Cosmochim. Acta 59, 443–453. doi:10.1016/0016-7037(94)00381-U
632

8. APPENDIX A

Appendix A contains the schematic for the rocking autoclave system from Coretest Systems, Inc. (Fig. A1) and the recipes for the synthetic brine created by Marcon et al. (2017) in Experiment 1, as well as our NaCl brine created for Experiment 2 in Table A1. Table A2 contains the generalized composition of the synthetic fracturing fluid created and provided by Paula Mouser at The Ohio State University used for both Experiment 1 and 2. The table itself is reproduced from Kekacs et al. (2015) and Marcon et al. (2017).

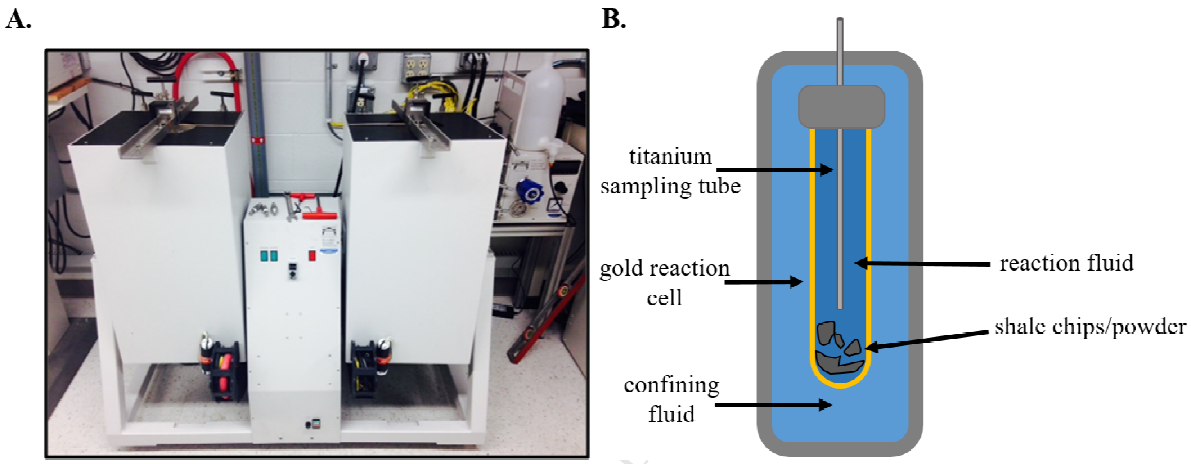

Figure A1: (A.) R-1-001 Dual-Furnace Rocking Autoclave (RAC) setup from Coretest Systems, Inc. in the HiPIR Transport laboratory at NETL Albany. The vessels are constantly rotated from the vertical to the horizontal positions to keep the reaction vessels well-mixed. (B.) A schematic of the setup of the reaction vessel showing the reaction fluid and shale chips/powder sealed in the gold reaction cell which is itself set in the main body filled with water. A titanium sampling tube accessing the gold reaction cell permits the fluids to be drawn off and sampled while the system is still under high pressure and temperature.

Table A1: Composition of synthetic brines used in Experiments 1 and 2

	mass added to 1 L solution g
*Experiment 1**	
$CaCl_2$	3
$MgCl_2$	0.1
Na_2SO_4	0.001
Na_2CO_3	1
KCl	0.2
NaCl	44
Si (1000 mg/L sol'n)	0.17
Fe (200 mg/L sol'n)	0.001
Experiment 2	
NaCl	44.5

*from Marcon et al. (2017)

Table A1: Generalized composition of synthetic fracturing fluid

General Composition of Synthetic Fracturing Fluid[c]

Chemical Additive	Disclosed Ingredients	[mass (g) or volume (mL)]/L fluid
Carrier/base fluid	Source water (collected from Atwood Lake in Senecaville, OH)	896 ml
Proppant	Sand (100 mesh sand produced by Unimin)	99 g
Acid	HCl (15% by mass)	3.5 g
Fe control	Citric acid	0.014 g
Corrosion inhibitor AI600[a]	Ethylene glycol, dimethyl formamide, decanol, isopropanol, octanol, 2-butoxyethanol, ethoxylated nonylphenols, cinnamaldehyde, tar bases, quinoline derivatives, benzyl chloride (quaternized), triethyl phosphate	0.007 ml
Friction reducer WFR-61LA[a]	Petroleum distillate, sodium chloride, alcohol ethoxylated C12-16, quaternary ammonium chloride	0.12 ml
Surfactant Revert flow[a]	Alcohol ethoxylated, isoporopanol, citrusturpenes, alcohol ethoxylated (C6 - C12), DB-964 (polyoxyethylene-polyoxypropylene block polymer)	0.47 ml
Clay stabilizer CC-120[a]	Proprietary non-hazardous salt	0.44 ml
Gelling agent WGA 15L[a]	Petroleum distillate	0.52 ml
Biocide EC6110A[b]	Glutaraldehyde, quaternary ammonium compound, ethanol	0.05 ml
Cross linker	Ethylene glycol	0.008 g
Boric acid	0.004 g	
Ethanolamine	0.002 ml	
Breaker	Ammonium persulfate	0.005 g
pH adjustor	K_2CO_3	0.018 g
	KOH	0.007 g

[a]Weatherford Fracturing Technologies

[b]Nalco Company

[c]reproduced from Kekacs et al. (2015) and Marcon et al. (2017)

Highlights

- Simulated fracturing experiments with Marcellus shale show no major release of REEs
- REEs are likely not suitable as tracers for fracturing fluid/shale interaction
- REEs are likely not major byproducts of hydraulically fractured shales